ELSEVIER

Journal of Alloys and Compounds 323–324 (2001) 753–758

Journal of ALLOYS AND COMPOUNDS

www.elsevier.com/locate/jallcom

Optical properties of Er^{3+} ions in transparent glass ceramics

J. Méndez-Ramos[a,*], V. Lavín[a], I.R. Martín[a], U.R. Rodríguez-Mendoza[a], J.A. González-Almeida[a], V.D. Rodríguez[a], A.D. Lozano-Gorrín[b], P. Núñez[b]

[a]*Dpto. Física Fundamental y Experimental, Universidad de La Laguna, 38206 La Laguna, Tenerife, Spain*
[b]*Dpto. de Química Inorgánica, Universidad de La Laguna, 38206 La Laguna, Tenerife, Spain*

Abstract

A study of optical properties and upconversion processes among Er^{3+} ions in oxyfluoride glass and glass ceramic matrix has been carried out. From optical absorption spectra, the oscillator strengths have been obtained for several transitions and they have been used to calculate the Judd–Ofelt parameters. Experimental lifetime values are compared with those obtained with the Judd–Ofelt theory. Different upconversion emissions at 545, 660 and 800 nm have been obtained in Er^{3+} doped glass and glass ceramics by exciting at 975 nm. A systematic investigation of the green upconversion is reported with the purpose of determining the involved upconversion mechanisms.
© 2001 Published by Elsevier Science B.V.

Keywords: Glass ceramics; Er^{3+}; Optical properties; Upconversion; Energy transfer

1. Introduction

Oxyfluoride glasses have created much interest as host materials for active optical devices such as lasers and optical amplifiers which utilise f–f transitions of rare earth ions [1–3]. After a thermal treatment close to the crystallization temperature it is possible to obtain a glass–ceramic, in which fluoride nanocrystals are embedded in a primarily oxide glass matrix. Moreover, this glass ceramic remains highly transparent in spite of the high (20–30%) volume fraction of the nanocrystal phase. Thus, if the rare earth ions are incorporated into the crystalline phase, the oxyfluoride glass–ceramic combine the particular optical properties of these ions in fluoride hosts [4,5] with the elaboration and manipulation advantages of oxide glasses. A previous study with Eu^{3+}-doped SiO_2–PbF_2–CdF_2-based glass ceramic has shown that almost all rare-earth ions are in crystalline phase after thermal treatment [6].

At present there is a great interest in luminescent materials for efficient frequency upconversion from infrared into visible radiation, mainly because a visible source pumped by a near infrared laser would be useful for high capacity data storage optical devices. In these upconversion processes, excited state absorption (ESA) and energy transfer (ET) involving rare earth ions in a solid matrix may present very large efficiencies. A lot of work has been devoted to upconversion lasers involving Er^{3+} ions by exciting the $^4I_{9/2}$, $^4I_{11/2}$ or $^4I_{13/2}$ levels at 0.80, 0.98 and 1.5 μm, respectively. Different schemes based on ESA or ET have been proposed for the $^4S_{3/2}$ and $^4F_{9/2}$ levels to produce, respectively, green and red output [7–10].

It is known that oxyfluoride glass–ceramics doped with Er^{3+} present an increased upconversion efficiency relative to the precursor glasses by a factor of about 100 [1]. In this work the optical properties of the Er^{3+} ions in SiO_2–PbF_2–CdF_2-based glasses and glass ceramics are analysed with the main goal of determining the mechanisms involved in the upconversion processes in these matrices.

2. Experimental

The samples used in this study were prepared with the following composition in mol%: 30 SiO_2, 15 Al_2O_3, 29 CdF_2, 22 PbF_2, $(4-x)$ YF_3 and x ErF_3; $x=0.1$ and 2.5. The final glass was obtained by melting at 1050°C for 2 h and finally casting the melt into a slab on a stainless steel plate at room temperature. The transparent oxyfluoride glass ceramics were obtained just by thermal treatment of the glass at 470°C for 24 h to precipitate microcrystallites without loss of transparency. Optical absorption measurements were performed on a Perkin Elmer Lambda 9 spectrophotometer. Broadband emission spectra were obtained by exciting the samples with light from a 250 W incandescent lamp passed through a 0.25 m mono-

---

*Corresponding author.

PII: S0925-8388(01)01077-5

chromator. Fluorescence was detected through a 0.25 m double monochromator with a photomultiplier. The spectra were corrected by the instrumental response. The measurements of emission temporal evolution were carried out with a tunable dye laser as excitation source with typical pulses of 1 mJ during 5 ns. This laser was pumped by the 532 nm pulsed light from a doubled Nd-YAG laser. The fluorescence was recorded using a digital storage oscilloscope controlled by a personal computer. For stationary upconversion measurements, a 975-nm laser diode beam with a power up to 150 mW focused over a surface of 2.5 mm^2 was used as excitation source while, for pulsed upconversion measurements, an optical parametric oscillator (OPO) sintonized at 975 nm was utilised. The incident radiation power was measured by a Gentec TPM-300 Power meter.

3. Theoretical background

From the absorption spectrum, the oscillator strengths of the electronic transitions can be calculated using the expression

$$f = \frac{mc}{\pi e^2 N}\int \frac{2.303\mathrm{OD}(\nu)}{d}\,\mathrm{d}\nu \tag{1}$$

where m and e are the electron mass and charge, respectively, c is the light velocity, N is the number of absorbing ions in the unit volume, ν is the light frequency, OD(ν) is the optical density and d is the thickness of the sample.

In the Judd–Ofelt theory [11,12] the oscillator strength of the aJ→bJ′ transition (at mean frequency ν) is given by

$$f(\mathrm{aJ,bJ'}) = \frac{8\pi^2 m\,\nu}{3h(2J+1)e^2 n^2}[X_{\mathrm{ed}}S_{\mathrm{ed}}(\mathrm{aJ,bJ'}) + X_{\mathrm{md}}S_{\mathrm{md}}(\mathrm{aJ,bJ'})] \tag{2}$$

where n is the refractive index of the host at the mean frequency of the transition, $X_{\mathrm{ed}} = n(n^2+2)^2/9$, $X_{\mathrm{md}} = n^3$ and, finally, S_{ed} and S_{md}, which give the electric and magnetic dipole contributions, respectively, can be written

$$S_{\mathrm{ed}} = e^2 \sum_{t=2,4,6} \Omega_t \left| \left\langle \mathrm{aJ}|U^{(t)}|\mathrm{bJ'}\right\rangle \right|^2 \tag{3}$$

$$S_{\mathrm{md}} = \left[\frac{e}{2mc}\right]^2 \left| \left\langle \mathrm{aJ}|L+2S|\mathrm{bJ'}\right\rangle \right|^2 \tag{4}$$

where the Ω_t parameters, known as Judd–Ofelt parameters, are characteristic of each ion–matrix combination. The reduced matrix elements of $L+2S$ and of the unit tensors $U^{(t)}$ are not very sensitive to the ion environment. The spontaneous emission probabilities A(aJ,bJ′) of the different electronic transitions are given in the Judd–Ofelt theory by

$$A(\mathrm{aJ,bJ'}) = \frac{64\pi^4\nu^3}{3hc^3(2J+1)}[X_{\mathrm{ed}}S_{\mathrm{ed}}(\mathrm{aJ,bJ'}) + X_{\mathrm{md}}S_{\mathrm{md}}(\mathrm{aJ,bJ'})] \tag{5}$$

and the radiative lifetime of an excited level aJ by

$$\tau = \frac{1}{\sum_{\mathrm{bJ'}} A(\mathrm{aJ,bJ'})} \tag{6}$$

where the sum is extended over all the states at energies lower than aJ.

When the interactions between luminescent ions are not important the photoluminescence decay curves can be fitted to a single exponential. However, when the concentration is large enough, energy transfer appears and the decay curves become non exponential. In order to compare different curves, it is useful to calculate an averaged lifetime with the equation

$$\left\langle \tau \right\rangle = \frac{\int_0^\infty I(t)\,\mathrm{d}t}{I(0)} \tag{7}$$

4. Results and discussion

4.1. Optical absorption and lifetimes

The energy level diagram of Er^{3+} ions obtained in oxyfluoride glasses is presented in Fig. 1. From room-temperature absorption spectra of the Er^{3+} ions in glass and glass ceramic it is found that Stark components are better resolved in the glass ceramics, indicating that the ions go into a like crystalline environment by the heat treatment. The spectra for the transition $^4I_{15/2} \rightarrow {}^4S_{3/2}$ are

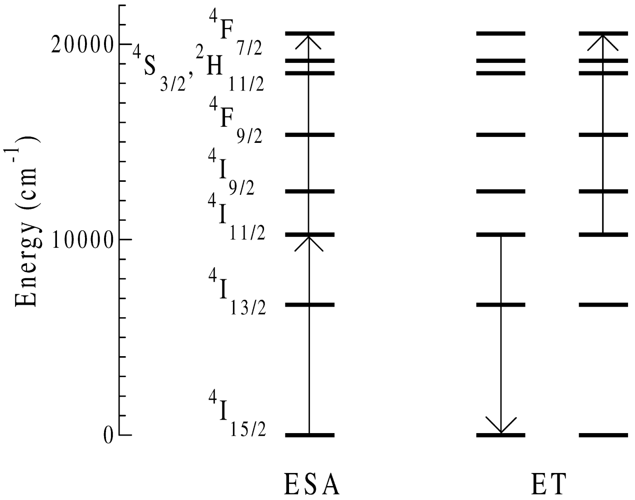

Fig. 1. Energy level diagram of Er^{3+} ions in an oxyfluoride glass. Upconversion mechanisms by excited state absorption (ESA) and energy transfer (ET) are indicated.

Table 1
Experimental and calculated oscillator strengths ($\times 10^{-8}$) in Er^{3+} doped glass and glass ceramic samples. All transitions are from the $^4I_{15/2}$ level (glass rms$=5.7\times 10^{-7}$; glass ceramic rms$=5.9\times 10^{-7}$)

Levels	Glass			Glass ceramic		
	λ (nm)	f_{exp}	f_{cal}	λ (nm)	f_{exp}	f_{cal}
$^4I_{13/2}$	1536	224	135.4	1513	246.9	149.2
$^4I_{11/2}$	979	50.1	65.1	978	64.5	64.9
$^4I_{9/2}$	799	47.6	26.8	802.5	50.9	18.1
$^4F_{9/2}$	651.5	272.6	199.9	652.5	248.4	176.7
$^4S_{3/2}$	543	43.2	52.5	541.5	49	60.8
$^2H_{11/2}$	521	770.5	783.4	523.5	351	347.2
$^4F_{7/2}$	488.5	201.9	203.2	487.5	206.1	216.1
$^4F_{5/2}$, $^4F_{3/2}$	451	72.8	99.5	450	91.6	115.1
$(^2G\ ^4F\ ^2H)_{9/2}$	406	59	75.5	406	53.5	83.4
$^4G_{11/2}$	378	1389	1379.5	380	610.4	610.4
$^4G_{9/2}\,^2K_{11/2}\,^2G_{7/2}$	365	128.9	233.9	364.5	101.2	203.9

similar to those presented by Mortier and Auzel for this transition [3], with an also similar increase, about 100%, of the maximum absorption cross-section.

With these spectra and using Eq. (1) the experimental oscillator strengths were calculated, assuming the same value for the refractive index [2]. In the results, given in Table 1, there are important changes from glass to glass ceramics matrix in the hypersensitive transition to the levels $^2H_{11/2}$ and $^4G_{11/2}$. The experimental oscillator strengths were used to determine the Judd–Ofelt parameters by a least squares fitting to Eq. (2). The reduced matrix elements of the $U^{(t)}$ and $L+2S$ operators given by Carnall et al. for Er^{3+} [13] have been used in our calculations. The obtained Judd–Ofelt parameters are presented in Table 2 and the transition probabilities, calculated from these parameters, are shown in Table 3.

It is interesting to analyse the decay mechanism of the $^4S_{3/2}$ level because of its role in upconversion processes. The lifetime of this level depends on its thermalization with the $^2H_{11/2}$ level. The effective radiative-emission probability for these two levels may be calculated considering an energy separation of 777 cm^{-1} in the glass and 635 cm^{-1} in the glass ceramic, obtained from optical absorption data presented in Table 1. In this way, similar values of 384 and 374 μs are obtained for the radiative lifetime of the $^4S_{3/2}$ ($^2H_{11/2}$) thermalized levels in the glass and in the glass ceramic, respectively. Lifetime measurements for these levels give lower values, about 132 μs in the glass and about 232 μs in the glass ceramic doped with 0.1 mol% of Er^{3+} (Table 2), indicating that non radiative deexcitation probabilities are appreciable. The higher value for the glass ceramic could be explained on basis to the lower lattice vibration energies at the sites occupied by the Er^{3+} ions in this matrix. When the dopant concentration is increased from 0.1 to 2.5 mol%, resonant energy transfer processes become important in the deexcitation of the $^4S_{3/2}$ ($^2H_{11/2}$) levels and the decays are faster. The decrease of the experimental average lifetime is more important in the glass ceramics, Table 2, as a consequence of the reduction of distances between Er^{3+} ions when they go into nanocrystals.

The other important level in upconversion emission excited at 975 nm is $^4I_{11/2}$. In glass and glass ceramic doped with 0.1 mol% of Er^{3+} this level presents experimental lifetimes of about 4 ms, close to those calculated from the radiative probabilities in Table 3. It is remarkable that when the Er^{3+} concentration increases to 2.5 mol%, the average lifetime of the $^4I_{11/2}$ level is strongly decreased by non resonant energy transfer towards ions in the ground state. In this way, a very short averaged lifetime of 55 μs is obtained for the glass whereas the result for the glass ceramic is 565 μs.

Table 2
Judd–Ofelt parameters Ω_t, calculated radiative lifetimes τ and experimental averaged lifetimes $\langle\tau\rangle$ for different levels in Er^{3+} doped glass and glass ceramic

Levels	Ω_2	Ω_4	Ω_6	$^4S_{3/2}$ ($^2H_{11/2}$)		$^4I_{11/2}$	
				τ	$\langle\tau\rangle$	τ	$\langle\tau\rangle$
Glass	$4.34{*}10^{-20}$	$1.16{*}10^{-20}$	$1.16{*}10^{-20}$	384 μs	132 μs[a] 4.6 μs[b]	4.6 ms	4.1 ms[a] 55 μs[b]
Glass ceramic	$1.68{*}10^{-20}$	$7.70{*}10^{-21}$	$1.34{*}10^{-20}$	374 μs	232 μs[a] 1.0 μs[b]	4.6 ms	4.0 ms[a] 565 μs[b]

[a] With 0.1 mol% of Er^{3+}.

[b] With 2.5 mol% of Er^{3+}.

Table 3
Transition probabilities calculated from Judd–Ofelt parameters for glass and glass ceramic samples doped with Er^{3+} ions. The magnetic dipole probabilities are also included

Transition	λ(nm)	Glass		Glass ceramic	
		A_{ed} (s^{-1})	A_{md} (s^{-1})	A_{ed} (s^{-1})	A_{md} (s^{-1})
$^4I_{13/2} \rightarrow {}^4I_{15/2}$	1532	135.1	38.5	146.5	38.5
$^4I_{11/2} \rightarrow {}^4I_{13/2}$	2780	22.5	8.9	23.1	8.9
$^4I_{15/2}$	977	186.2		185.5	
$^4I_{9/2} \rightarrow {}^4I_{11/2}$	4530	1.0	1.3	1.0	1.3
$^4I_{13/2}$	1723	58.9		67.7	
$^4I_{15/2}$	802	135.5		92.2	
$^4F_{9/2} \rightarrow {}^4I_{9/2}$	3443	4.9		2.1	
$^4I_{11/2}$	1956	86.4		88.1	
$^4I_{13/2}$	1148	76.9		59	
$^4I_{15/2}$	660	1546.5		1368.8	
$^4S_{3/2} \rightarrow {}^4F_{9/2}$	3178	0.7		0.9	
$^4I_{9/2}$	1652	77.5		80.7	
$^4I_{11/2}$	1211	48.3		54.5	
$^4I_{13/2}$	844	595.5		688.1	
$^4I_{15/2}$	545	1479.7		1709.7	
$^2H_{11/2} \rightarrow {}^4F_{9/2}$	2643	27.2		10.7	
$^4I_{9/2}$	1495	112.7		68.3	
$^4I_{11/2}$	1124	75.7		45.7	
$^4I_{13/2}$	800	136.7		90.8	
$^4I_{15/2}$	523	7815.9		3480.3	

4.2. Upconversion processes

By exciting at 975 nm ($^4I_{15/2} \rightarrow {}^4I_{11/2}$) upconversion emissions at 545, 660 and 800 nm are obtained in oxyfluoride glass and glass ceramic doped with 2.5 mol% of Er^{3+}, the spectra are presented in Fig. 2. The upconversion luminescence intensities of the heat treated sample are stronger than those of precursor glasses by an important factor of about 1000. Under 800 nm laser excitation, Takahashi et al. [14] also observed an enhancement of the upconversion efficiency with heat treatment by a factor of 100–200. As can be noticed in Fig. 2, upconversion emission bands become sharper and the components are better resolved as the ceramming process is carried out.

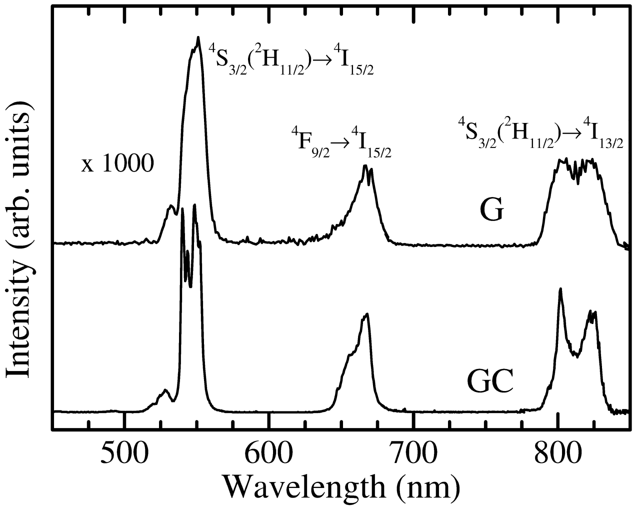

Fig. 2. Upconversion emission spectra obtained exciting at 975 nm at room temperature an oxyfluoride glass (G) and a glass ceramic sample (GC) doped with 2.5 mol% of Er^{3+}.

In upconversion processes the emission intensity I_{UP} will be proportional to a power n of the IR excitation intensity I_{IR}, i.e.

$$I_{UP} \propto (I_{IR})^n,$$

where n is the number of IR photons absorbed per visible photon emitted. A plot of logarithm of I_{UP} versus logarithm of I_{IR} should yield a straight line with slope n. Such a plot for the 545 nm upconversion emission corresponding to excitation at 975 nm is shown in Fig. 3 for the glass ceramic. A value of 1.94 is obtained for the slope in this matrix and a similar result, close to 2, was obtained for the glass, indicating that the $^4S_{3/2}(^2H_{11/2})$ level is populated by a two photon process in both samples. In this way, two possible mechanisms, shown in Fig. 1, can produce the upconversion emission at 545 nm:

(i) After a first excitation to the $^4I_{11/2}$ level, a second photon is absorbed by the same ion (ESA): $^4I_{15/2} \xrightarrow{h\nu} {}^4I_{11/2} \xrightarrow{h\nu} {}^4F_{7/2}$

(ii) An excited ion transfers energy to another excited

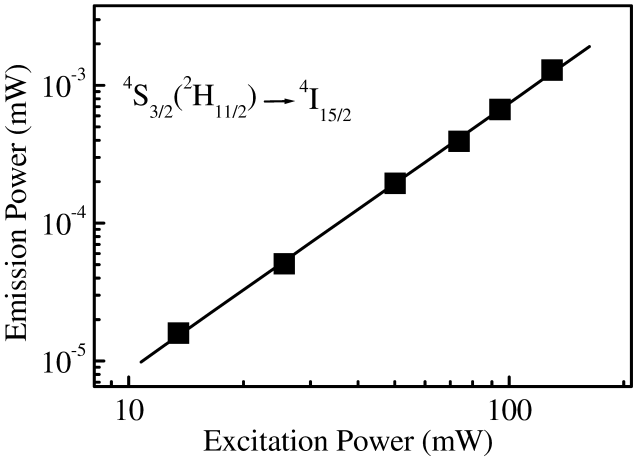

Fig. 3. Dependence of the upconversion emission at 545 nm on excitation power at 975 nm in the glass ceramic sample doped with 2.5 mol% of Er^{3+} at room temperature. The solid line corresponds to a straight line fit with a slope of 1.94.

ion according to the following resonant channel (ET): $(^4I_{11/2}, {}^4I_{11/2}) \rightarrow (^4I_{15/2}, {}^4F_{7/2})$.

Both upconversion mechanisms excite the Er^{3+} ions to the $^4F_{7/2}$ level, from this level the $^4S_{3/2}(^2H_{11/2})$ levels are populated by multiphonon deexcitation.

Additional information in order to determine the upconversion mechanism can be obtained analysing the dynamics of the upconversion emissions under pulsed IR excitation. The temporal evolution of the upconversion emission at 545 nm by exciting with a laser pulse at 975 nm glass and glass ceramic samples doped with 2.5 mol% of Er^{3+}, presented in Fig. 4, shows very different behaviours. In the glass sample, the maximum of the upconversion emission is reached within the pulsed excitation. This decay is similar to the one obtained by direct excitation to the $^4S_{3/2}(^2H_{11/2})$ levels (about 4.6 μs), indicating that, for the glass sample, the Er^{3+} ions are mainly excited to the $^4F_{7/2}$ level during the laser pulse and therefore the ESA upconversion mechanism predominates over the energy transfer. However, slow rise and decay are observed in the glass ceramic sample. This result can be explained on the basis of the ET upconversion mechanism considering the longer lifetime of the $^4I_{11/2}$ level in the glass ceramic (565 μs) and the increased resonant energy transfer probabilities between ions excited to the $^4I_{11/2}$ level by the shortening of the distances between Er^{3+} ions.

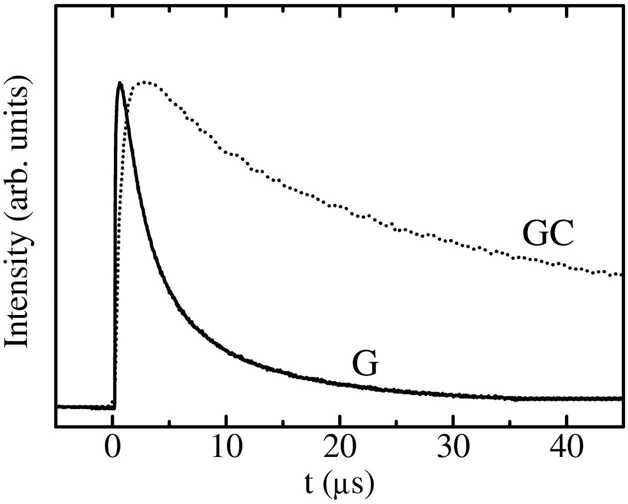

Fig. 4. Temporal evolution of the upconversion emission at 545 nm obtained at room temperature under pulsed excitation at 975 nm in a glass (G) and in a glass ceramic sample (GC) doped with 2.5 mol% of Er^{3+}.

5. Conclusions

From optical spectroscopy measurements in oxyfluoride glass and glass ceramic doped with Er^{3+}, important changes in spectra and lifetimes due to the ceramming process have been observed, suggesting that the rare earth ions have entered into a crystalline phase. Upconversion emissions at 545, 660 and 800 nm are obtained in the glass sample after excitation to the $^4I_{11/2}$ level at 975 nm. The intensities of these emissions are increased by a factor of 1000 through the heat treatment. In the glass, the dominant upconversion mechanism is ESA whereas, in the glass ceramic, the longer averaged lifetime of the $^4I_{11/2}$ level and the increasing of the resonant energy transfer processes between ions excited to this level favour a much more efficient ET process.

Acknowledgements

This work was partially supported by 'Gobierno Autónomo de Canarias (PI1999/100)', 'Comisión Interministerial de Ciencia y Tecnología (PB98-0437)' and 'FEDER program and Comisión Interministerial de Ciencia y Tecnología (1FD97-1422)'.

References

[1] Y. Wang, J. Ohwaki, Appl. Phys. Lett. 63 (1993) 3268.
[2] P.A. Tick, N.F. Borrelli, L.K. Cornelius, M.A. Newhouse, J. Appl. Phys. 78 (1995) 6367.
[3] M. Mortier, F. Auzel, J. Non-Cryst. Solids 256–257 (1999) 361.
[4] V. Lavín, V.D. Rodríguez, I.R. Martín, U.R. Rodríguez-Mendoza, J. Lumin. 72–74 (1997) 437.
[5] V.D. Rodríguez, V. Lavín, U.R. Rodríguez-Mendoza, I.R. Martín, Opt. Mater. 13 (1999) 1.
[6] J. Méndez-Ramos, V. Lavín, I.R. Martín, U.R. Rodríguez-Mendoza, V.D. Rodríguez, A.D. Lozano-Gorrín, P. Nuñez, in: Recontre Franco-Espagnole sur la chimie et physique de l'etat solide, Carcans-Maubuisson, Mars, 2000.
[7] S.A. Pollack, D.B. Chang, N.L. Moise, J. Appl. Phys. 60 (1986) 4077.
[8] N.J. Cockroft, G.D. Jones, D.C. Nguyen, Phys. Rev. B 45 (1992) 5187.
[9] M.P. Hehlen, G. Frei, H.U. Gudel, Phys. Rev. B 50 (1994) 16264.

[10] Cid B. de Araújo, L.S. Menezes, G.S. Maciel, L.H. Acioli, A.S.L. Gomes, Y. Messaddeq, A. Florez, M.A. Aegerter, J. Appl. Phys. 68 (1996) 602.
[11] B.R. Judd, Phys. Rev. B 127 (1962) 750.
[12] G.S. Ofelt, J. Chem. Phys. 37 (1962) 511.
[13] W.T. Carnall, Argonne National Laboratory Report ANL-78-XX-95 (1978).
[14] M. Takahashi, Y. Kawamoto, M. Uzuki, R. Kanno, J. Appl. Phys. 83 (1998) 3920.